ISSN 0965-545X, Polymer Science, Series A, 2018, Vol. 60, No. 2, pp. 141–155. © Pleiades Publishing, Ltd., 2018.

SOLUTIONS

Fast Crystallization and Toughening of Poly(*L*-lactic acid) by Incorporating with Poly(ethylene glycol) as a Middle Block Chain[1]

Xueyan Yun, Xiaofang Li, Ye Jin, Wenxiu Sun, and Tungalag Dong*

College of Food Science and Engineering, Inner Mongolia Agricultural University, Hohhot, Inner Mongolia, 010018 China

**e-mail: dongtlg@163.com*

Received March 12, 2017;
Revised Manuscript Received July 31, 2017

Abstract—High molecular weight poly(*L*-lactic acid)-poly(ethylene glycol)-poly(*L*-lactic acid) (PLLA–PEG–PLLA; PLGL) triblock copolymers with various lengths of the PLLA blocks were synthesized by ring-opening polymerization of *L*-lactide. The amorphous and crystalline PLLA and PLGL films were prepared by hot pressing with different temperature treatments. PLLA and PEG blocks exhibited good miscibility in the amorphous PLGL samples, while phase separation occurred in the crystalline ones. The flexible PEG blocks not only accelerated the crystallization rate of PLLA but also greatly improve its flexibility. The crystallization time of PLGL copolymers shorten to less than 5 min and copolymers showed much better flexibility than neat PLLA, the maximum fracture strain reached about 600% for amorphous sample. The processing time of PLLA was greatly shortened and the brittleness of material was improved.

DOI: 10.1134/S0965545X18020141

INTRODUCTION

The universal use of non-degradable plastic products has caused serious environmental pollution. One of the most effective ways to solve the problem is the development of biodegradable polymers. Among these biodegradable polymers, poly(*L*-lactic acid) (PLLA) is one of the most important polyesters that are derived from renewable biomass such as corn and sugar beets [1]. It is known for its biocompatibility, low toxicity and immunogenicity and resorbability through natural pathway [2, 3], and it has a variety of application in many fields such as drug delivery [4, 5], tissue engineering [6], food packaging [7–9]. For a wide commodity applications, a good material must have good mechanical and processability. However, the disadvantages of poor mechanical properties and slow crystallization rate of PLLA limit its wide application. PLLA has a glass transition temperature well above room temperature, it was in glassy state at room temperature and was a rather brittle and rigid polymer, the elongation ratio is only about 5%. Crystallinity, if developed, increases the elastic modulus and further enhance the brittleness [10, 11]. Considerable efforts have been made to improve the mechanical properties of PLLA, such as blending, copolymerization and plasticization [12–17].

Plasticizers are widely used in the plastics industry to improve processability, flexibility and ductility of glassy polymers [18]. PLLA was plasticized with various plasticizers and their efficiency were evaluated in two aspects: one is the shift of glass transition temperature T_g, the other is the improvement mechanical properties [19]. Poly(propylene glycol) (PPG) and poly(ethylene glycol) (PEG) were found to be efficient plasticizers for PLLA [20–27], the elongation at break of PLLA was greatly increased. PLLA was melt-blended with an ethylene glycol/propylene glycol random copolymer poly(ethylene glycol-*co*-propylene glycol) (PEPG) [28]. With 5~20% PEPG additive, the toughness increased. PLLA was plasticized with triphenyl phosphate and the results showed that the crystallinity of plasticized PLLA markedly increased when compared with neat PLLA [29]. Oligomeric lactic acid, glycerol, epoxidized palm oil, and partial fatty acid eaters also have been used as plasticizers for PLLA [30, 31].

The fully biodegradable PLLA and poly(ethylene succinate) (PLLA/PES) blends were obtained via melt-blending. The tensile test result showed that the elongation at break of PLLA/10 wt % PES blend can be increased by about four times, while keeping considerably high strength and modulus [14]. While a blend with 10 wt % of poly(ester-urethane) can be drawn to more than 300% [13]. A series of organic-inorganic hybrid films were prepared based on octa(3-chloropropylsilsesquioxane) (OCPS) and PLLA via simple solution blending method. The yield strain of OCPS/PLLA hybrid films increased to 91% with 15%

[1] The article is published in the original.

OCPS additive [32]. The elongation at break of PLLA/Hydrolysate blend films was increased to 400% [33]. Two kinds of polyesters containing 2-pyrone-4, 6-dicarboxylic acid (PDC) moieties in PLLA and poly(butylene succinate) (PBS) main chains were employed as an additive to PLLA for the improvement of elongation [34]. The mechanical properties of composites of PLLA and double-fullerene end-capped PEG were investigated, and the fracture strain of the composites aged at room temperature increased by astonishing 100 times [35].

Poly(vinyl alcohol)-*graft*-(lactic acid) (PVA-*g*-LA) copolymer has better thermal stability and exhibits higher elongation at break [36, 37]. PLLA–PBS–PLLA triblock copolyesters with different PLLA and PBS chain length were synthesized and the segmental flexibilities of the hard PLLA blocks were found to be remarkably enhanced by the more flexible PBS block partner [38]. When poly(ethylene-*co*-butylene) (PEB) as a middle block chain incorporated in PLLA, the strain of PLLA–PEB–PLLA can reach more than 300% [39]. It was reported that increased the caproyl units in the poly(*L*-lactic acid-*co*-caprolactone) by a few percent substantially can increase the elongation of PLLA. In fact, some flexible polymers or monomers, such as poly(ε-caprolactone) (PCL) and PEG, play role of plasticizers in PLLA blends [20, 40–42]. The role of the plasticizer is to reduce the modulus of elasticity and enhance the segmental mobility, thus increasing the ability of amorphous PLLA to the plastic deformation [43]. The transition from brittle to ductile behavior in the plasticized PLLA occurs when T_g shifts to low temperature. The plastic deformation ability of PLLA was reflected in a decrease of yield stress and an increase of elongation at break.

The crystallizability and crystallinity of crystalline polymers are also the most important characteristics from the standpoint of practical applications; the characteristics strongly affect the processability and productivity of mold processing and performance of molded articles [44, 45]. PLLA is a kind of semi-crystalline polymer, the crystallization of PLLA is slow, which is also not convenient for processing [46, 47]. A series of nucleating agent for PLLA have been prepared to accelerate the crystallizing process of PLLA, including Talc, PLLA/PDLA stereocomplex crystallites, PDLA, nano-clay, cyclodextrin complex, compounds with hydrazide groups, benzoylhydrazide type and functionalized multiwalled carbon nanotubes, etc. [40, 47–61].

Although the addition of nucleating agents or the other polymers can be beneficial to the rate of polymer crystallization, the strength and modulus of blends are always reduced dramatically, and the embrittlement of the blends occurs due to incompatibility or the migration of these low molecular weight plasticizers from the bulk matrix to the surface [12, 62]. To obtain toughened products, both plasticizers and nucleating agent have been added to PLLA at the same time [61, 63, 64].

As far as we know, PEG was considered a good plasticizer for PLLA, the hydrophility, crystallization behavior, melting behavior and its application in drug release of PLLA–PEG diblock or triblock copolymers were always been investigated in most works. The molecular weight of most PLLA–PEG copolymer been investigated in most works are not more than 50000 and the molecular weight of PEG are always range from 400~4000. However, few works reported the crystallization behaviors and mechanical properties of high molecular weight PLLA–PEG–PLLA (PLGL) triblock copolymer.

For further use in food packaging, both the crystallinity and toughness of PLLA need to be further improved. Soft PEG segment was used to accelerate the crystallization rate and improve the toughness of PLLA in this study. To avoid the migration of PEG from the plastic result in lower the mechanical properties of packaging film and the contamination of foods, high molecular weight PLLA–PEG–PLLA triblock copolymers with various PLLA lengths was synthesized by copolymerization. The plasticization and fast crystallization effects of PEG block in PLLA based copolymers, as well as the mechanical properties of copolymers were investigated.

EXPERIMENTAL

Sample Preparation

Synthesis and characterization of PLLA–PEG–PLLA copolymers. *L*-lactide (>99.9%) was purchased from Purac Co. (Gorinchem, the Netherlands) and purified by recrystallization from ethyl acetate. PEG with a 2×10^4 molecular weight was obtained from SIGMA. Stannous octoate ($Sn(Oct)_2$), chloroform and methanol were purchased from Sinopharm Chemical Reagent Co., Ltd, China.

The PLGL triblock copolymers were prepared by ring-opening polymerization of *L*-lactide in the presence of PEG. Stannous octoate ($Sn(Oct)_2$) was used as a catalyst. For example, to synthesize the PLLA–PEG–PLLA (75000-20000-75000) triblock copolymer, PEG (2.67 g, 0.134 mmoL, $M_n = 2 \times 10^4$) was put into a 3-neck flask and vacuum dried at 100°C for 4 h. *L*-lactide (20 g, 0.25 mmol) and stannous octoate (0.06 g, 0.148 mmol) were added to the reaction mixtures and stirred at 120°C for 24 h under an argon gas ambience. The product was dissolved in chloroform and precipitated in excess cold methanol and the white precipitation was air dried in a fume hood and then vacuum dried at room temperature over 72 h.

In order to be simple, the samples were recorded as PLGL7, PLGL5, PLGL3 and PLGL2, respectively. The numbers after PLGL denote the supposed molecular weight/10000 of PLLA blocks, respectively.

Table 1. Molecular Characteristics of PLLA and PLGL triblock copolymers

Samples	Fitting ratio of EG/LA[c]	PLLA–PEG–PLLA[a]	EG/LA[a]	W_{PEG}[a], wt %	$M_{n,NMR}$[a], kDa	$M_{n,GPC}$[b], kDa	Pd[b]
PLLA	–	–	–	–	–	92.1	2.12
PLGL7	1/7.5	$(LA)_{77k}$–$(EG)_{20k}$–$(LA)_{77k}$	1/7.7	11.5	173.2	101.9	2.09
PLGL5	1/5.5	$(LA)_{58k}$–$(EG)_{20k}$–$(LA)_{58k}$	1/5.8	14.8	135.2	96.9	1.37
PLGL3	1/3.5	$(LA)_{37k}$–$(EG)_{20k}$–$(LA)_{37k}$	1/3.7	21.4	93.3	77.6	1.34
PLGL2	1/2.5	$(LA)_{28k}$–$(EG)_{20k}$–$(LA)_{28k}$	1/2.8	26.2	76.3	60.9	1.51

[a] Determined by ^{1}H NMR based on ethylene glycol (EG) unit (4H, 3.6 ppm) and *L*-lactic acid (LA) unit (1H, 5.09 ppm) of the PLGL copolymers. LA_x–EG_y–LA_x : x is the M_n of PEG midblock and y is the M_n of PLLA.
[b] Determined by GPC.
[c] Fitting ratio of EG/LA was a weight ratio in feed.

The molecular weight and the polydispersity were determined by gel permeation chromatography. The copolymer composition was evaluated with ^{1}H NMR. ^{1}H NMR signals of PLGL, δ_H, ppm: 5.09 (–COCH(CH_3)O–), 1.6 (–CH_3), 3.6 (–OCH_2CH_2–). The molecular weight of the PLLA block in the copolymer was determined from the copolymer composition on the basis of PEG's molecular weight. The molecular weights and compositions of copolymers together with the neat PLLA used for the experiments are listed in Table 1.

Preparation of PLLA–PEG–PLLA films. The samples for all characterizations were molded in a heated press at 200°C for 2 min without any applied pressure. After this period, a pressure of 30 MPa was applied for 2 min, and then the press plates of amorphous samples were quickly cooled to room temperature and the crystallized samples were then put into an incubator chamber at 90°C immediately and kept at this temperature until the samples were fully crystallization.

Characterization of PLGL Copolymers and Films

Nuclear magnetic resonance (NMR). ^{1}H NMR spectra of the polymers were recorded on a 400 MHz Bruker Advance 2B spectrometer with deuterated chloroform ($CDCl_3$) or deuterated trifluoroacetic acid (d-TFA) as the solvent.

Gel permeation chromatography (GPC). Molecular weights were measured on a gel permeation chromatography (GPC, Waters Co., Milford, MA, USA) consisting of a Waters degasser, a Waters 1515 isocratic HPLC pump, a Waters 2414 RI detector. THF was used as the eluent at a flow rate of 1.0 mL/min; the column temperature was 30°C.

The wide-angle X-ray diffraction (WAXD). WAXD patterns were recorded on a PW1830 (Philips Co., Holland). The CuK_α radiation (λ = 0.15418 nm) source was operated at 30 kV and 30 mA. All measurements were carried out at room temperature under atmospheric pressure. The scans were made between Bragg angles of 10 ~ 25° at a rate of 1.0 grad/min.

Differential scanning calorimetry (DSC). The isothermal crystallization and subsequent melting behavior of PLGL triblock copolymers as well as the neat PLLA were measured with differential scanning calorimetry (DSC Q20, TA Instruments, Co., USA) under a nitrogen purge. Each sample was weighed approximately 5~10 mg and encapsulated in an aluminum pan. Two different DSC heating process were used: First, the samples were initially scanned from 25 to 200°C with a heating rate of 10 grad/min; Second, the samples were initially scanned from 25 to –50°C and then heating to 200°C with a heating rate of 10 grad/min. Thermal parameters including T_g, melting temperature T_m, cold crystallization temperature T_{cc} and crystallization temperature T_c can be obtained from the thermal curves. The cold crystallization enthalpy ΔH_{cc}, crystallization enthalpy ΔH_c and melting enthalpy ΔH_m are calculated from the DSC curves when the samples were initially scanned from 25 to 200°C. The degree of crystallinity X_c was calculated from Eq. (1), ΔH_o is the enthalpy of polymers film with 100% crystallinity (PLLA: ΔH_o = 93 J/g; PEG: ΔH_o = 208 J/g) [46, 65].

$$X_C = \frac{\Delta H_m - \Delta H_{cc}}{\Delta H_o}. \quad (1)$$

Polarized light optical microscopy (POM). Nucleation and growth of PLLA spherulites were studied with a polarizing microscope (CaiKon, XPR-500C, Shanghai, China) coupled with a hot stage (CaiKon, KER 3100-08S, Shanghai, China). Those samples were prepared by hot pressing as well as the other samples used in other tests and firstly melting at 200°C for 2 min then quickly cooling to a fixed crystallization temperature at 100°C.

Dynamic mechanical thermal analysis (DMTA). Dynamic mechanical thermal analysis (DMTA) was made on a DMA (DMA Q800, TA Instruments, Co., USA) under the tensile mode. Each test sample was

30 mm long, 10 mm wide, and ca. 0.5 mm thick. The measurement was carried out at 5 Hz at a thermal scanning rate of 2 grad/min and the temperature was ranged from −120 to 200°C. The curves displayed storage modulus and tan theta (tan θ) versus temperature.

Tensile test. Measurement of mechanical properties of specimen was performed at room temperature with a universal tensile test machine (Xing Hui Electronics Co., LTD, Guangdong, China) at a crosshead speed of 50 mm/min. All samples were cut from the sheets and shaped into rectangular bar (ca. 0.3 mm thickness, 5 mm width and 28 mm length). Each value of mechanical properties reported was an average of five specimens.

Scanning electron microscopy (SEM). A scanning electron microscope (Shimadzu Co S-530, SEM, Japan) with an accelerating voltage of 15 kV was used to evaluate the morphology of fractured surfaces for the amorphous and crystallized samples after the tensile test. The samples were sputter-coated with gold particles up to a thickness of about 10 nm before the surface characterization.

RESULTS AND DISCUSSION

Molecular Characterization of PLGL Copolymers

The PLGL triblock copolymers with different PLLA chain lengths were prepared by ring opening polymerization of *L*-lactide on the PEG in the presence of stannous octoate as a catalyst. PEG ($M_n = 2 \times 10^4$) with two hydroxyl end groups was used as middle block; the principle of equal reactivity could be valid. Thus the PLLA blocks at both ends of a PLGL sample were assumed to have the same molecular weight. The total molecular weight and polydispersity (Pd) of the polymers, determined by GPC, and the results are shown in Table 1.

The relative molar ratio of EG/LA in copolymers determined by ^{1}H NMR were smaller than the fitting ratio, that may due to the incomplete reaction of monomers. All copolymers exhibited relative a higher molecular weight more than 7.6×10^4, which indicates a good film forming property. In addition, it also can be seen that the molecular weight decreased from 1.7×10^5 to 7.6×10^4 with the weight percentage of PEG in copolymers increasing from 11.5 to 26.2 wt %. The number molecular weights M_n of copolymers determined by GPC were smaller than that determined by ^{1}H NMR. This may because the systems contain some PLLA homo-polymers, which can lead higher molecular weights in NMR analysis. However, all polymers have relative small Pd values and indicate narrow molecular weight distributions. As a whole, both ^{1}H NMR and GPC results showed that high molecular weight PLGL copolymers with different PLLA chain lengths and PEG contents were successfully synthesized in this work.

WAXD Analysis

Two different temperature treats were used to prepared films by hot press. Amorphous samples were quickly cooled to room temperature after melting at 200°C while the crystallized samples were put into an incubator chamber at 90°C immediately and kept at this temperature until the samples were fully crystallization. WAXD was carried out to investigate the crystalline state of samples, and the results are shown in Fig. 1. Figure 1a shows the WAXD patterns of amorphous samples. It can be seen that no obvious diffraction peak was observed for neat PLLA, PLGL7 and PLGL5, which revealed a completely amorphous structure. With the increasing content of PEG block and the decreasing PLLA chain length, a broad diffraction peak at ca. 17.0° were observed in the WAXD patterns of PLGL3 and PLGL2 films, which indicates that most of the PLLA were in amorphous state and only a small amount crystallites existed for the processing condition [14].

It has been reported that depending on the crystallization, PLLA can crystallize in three different modifications (α, β and γ forms) [66]. Crystallization of PLLA from the melt or solution under normal conditions results in its most common and stable polymorph, α-form, with a 10/3 helical chain conformation where two chains are interacting in an orthorhombic unit cell [67]. Another new α'-form was also been believed to be existed and the α' crystal can transform into ordered α form during heating, and this transformation partly depended on the temperature and molecular weight of polymers [46, 67, 68].

Figure 1b demonstrated the WAXD patterns of the crystallized samples. Two diffraction peaks at 16.8° and 19.1° were observed for neat PLLA, indicating the PLLA crystalline sample adopts the α'-form crystal. In the case of PLGL7 copolymers, diffraction peaks were observed at 15.1°, 17.0°, 19.3° and 22.6°. The peaks of α'-form at 16.8° and 19.1° shifted to higher θ side, and new diffraction peaks at 15.1° and 22.6° were observed for all copolymers, indicating that the α crystal are mainly produced in PLGL copolymers [66]. This is to say, due to the presence of PEG and the change of molecular weight of PLLA block, the PLLA blocks form the α-form rather than the α'-form in PLGL copolymers when isothermal crystallized at 90°C [69–71]. However, here it failed to find clear crystal diffraction peaks of PEG in both amorphous and crystalline samples, indicating that the PEG blocks almost adopt the amorphous state.

Nonisothermal Crystallization Behavior

DSC analysis was performed to study the thermal behavior of polymers. Figure 2 shows the DSC traces

of PLLA and PLGL triblock copolymers with various PEG contents recorded during the heating scan from 25 to 200°C, and the thermal characteristics obtained from the curves are summarized in Table 2. As shown in Fig. 2a, The T_g, T_{cc} and T_m appeared at 59.5, 104.1 and 177.2°C in the amorphous PLLA, respectively. The DSC heating curve of amorphous PLLA also shows an enthalpy relaxation peak appeared at just above T_g and a small recrystallization peak at 157°C.

In the case of PLGL7, the similar T_g, T_{cc} and T_m correspond to PLLA blocks appeared at 43.0, 75.5 and 174.8°C, respectively, and these characteristic thermal transition temperature are lower than those of the neat PLLA. The enthalpy relaxation peak also appeared in the amorphous PLGL7 sample, the peak may be mistaken for melting peaks of the PEG. Furthermore, this endothermic peak becomes obviousness with increasing PEG content in amorphous PLGL copolymers, indicating that the endothermic peak was not attributed to melting of PEG, but the enthalpy relaxation peak of PLLA blocks. The recrystallization peaks also appeared in the PLGL samples, and the peak will disappear by the PEG content further increase in the other PLGL copolymers.

The amorphous PLLA showed the T_{cc} at 104.1°C with the ΔH_{cc} of 42.3 J/g, and the T_m at 177.2°C with the heat fusion of 44.1 J/g. On the basis of the values of cold crystallization and melting enthalpies, the crystallinity of amorphous PLLA was found to be only 1.9%, indicating that PLLA was difficult to crystallize at room temperature quenched from the melt.

With the increase of PEG contents, the T_{cc} of PLGL copolymers decreased firstly to 75.5°C then increased to 94.5°C for PLGL2 subsequently. This is due to the longer PEG chain length in the middle segment permits a higher mobility of the adjacent PLLA molecule chain, and result in acceleration of PLLA crystallization at low temperature. On the other hand, the T_{cc} values began to increase for the PLGL5, PLGL3 and PLGL2 samples with further increasing PEG content, indicating that the PEG block chain may also act as a mutual dilution effect and influence the crystallization process of PLLA blocks.

It can be seen from Table 2 that the as PEG increased, the T_ms of PLLA blocks for PLGL5~PLGL2 samples were further shifted to lower temperatures compared with neat PLLA. The ΔH_m of copolymers were lower than that of neat PLLA, and the X_c of PLLA blocks were gradually increased as increasing PEG block and decrease of the PLLA chain lengths. That may because on one hand the PEG in amorphous samples were in an amorphous state and had quite good mobility. On the other hand the shorter PLLA chain length also led to more mobility of molecular chains. Thus increased the chain mobility of PLLA and were more easily to gather to crystallization. It should be noticed that the X_c of PLLA blocks is

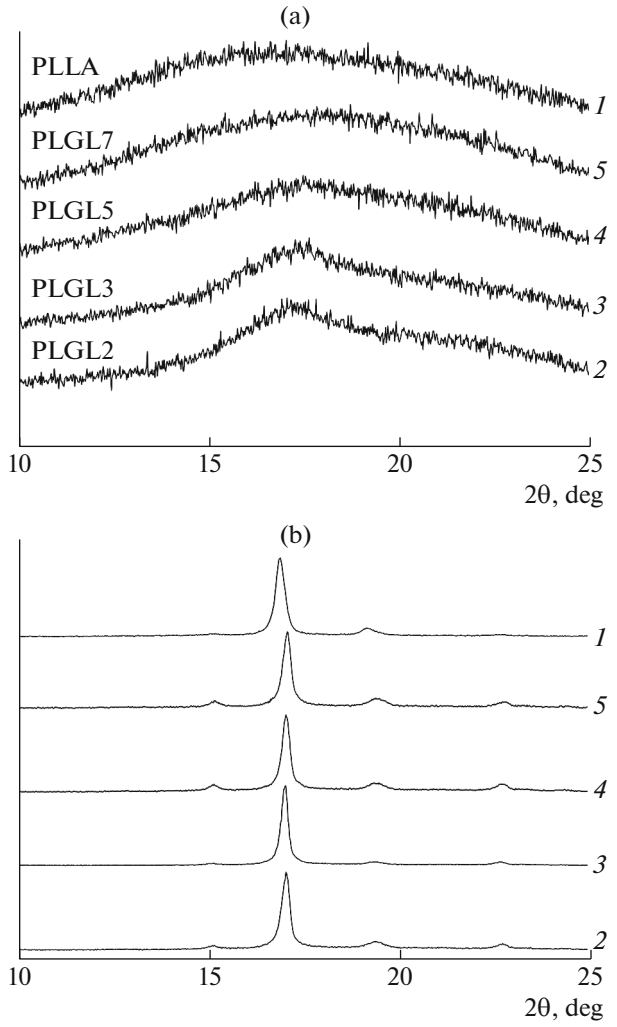

Fig. 1. WAXD patterns of (*1*) PLLA and PLLA–PEG–PLLA copolymers: (*2*) PLGL 2, (*3*) PLGL 3, (*4*) PLGL 5, (*5*) PLGL 7. (a) Amorphous samples quickly cooled at room temperature after melting at 200°C and (b) crystalline samples isothermally crystallized at 90°C after melting at 200°C.

very small and this is well consistent with the WAXD result, indicating an amorphous state of samples.

Here, it is noteworthy that the PEG blocks in the amorphous PLGL samples was completely free from the crystallization at room temperature as revealed by the DSC heating curves in the Fig. 2a. When the PLGL copolymers were directly cooled from the molten state to room temperature and then aged at room temperature for 3 days before the DSC measurement, no endothermal peak corresponding to the melting of the PEG crystalline phase was detected, suggesting that the PEG blocks were completely revealed from the crystallization under this condition.

Figure 2b depicts the DSC heating curves of crystallized PLLA and PLGL samples. Different with amorphous samples, no obvious peaks were observed

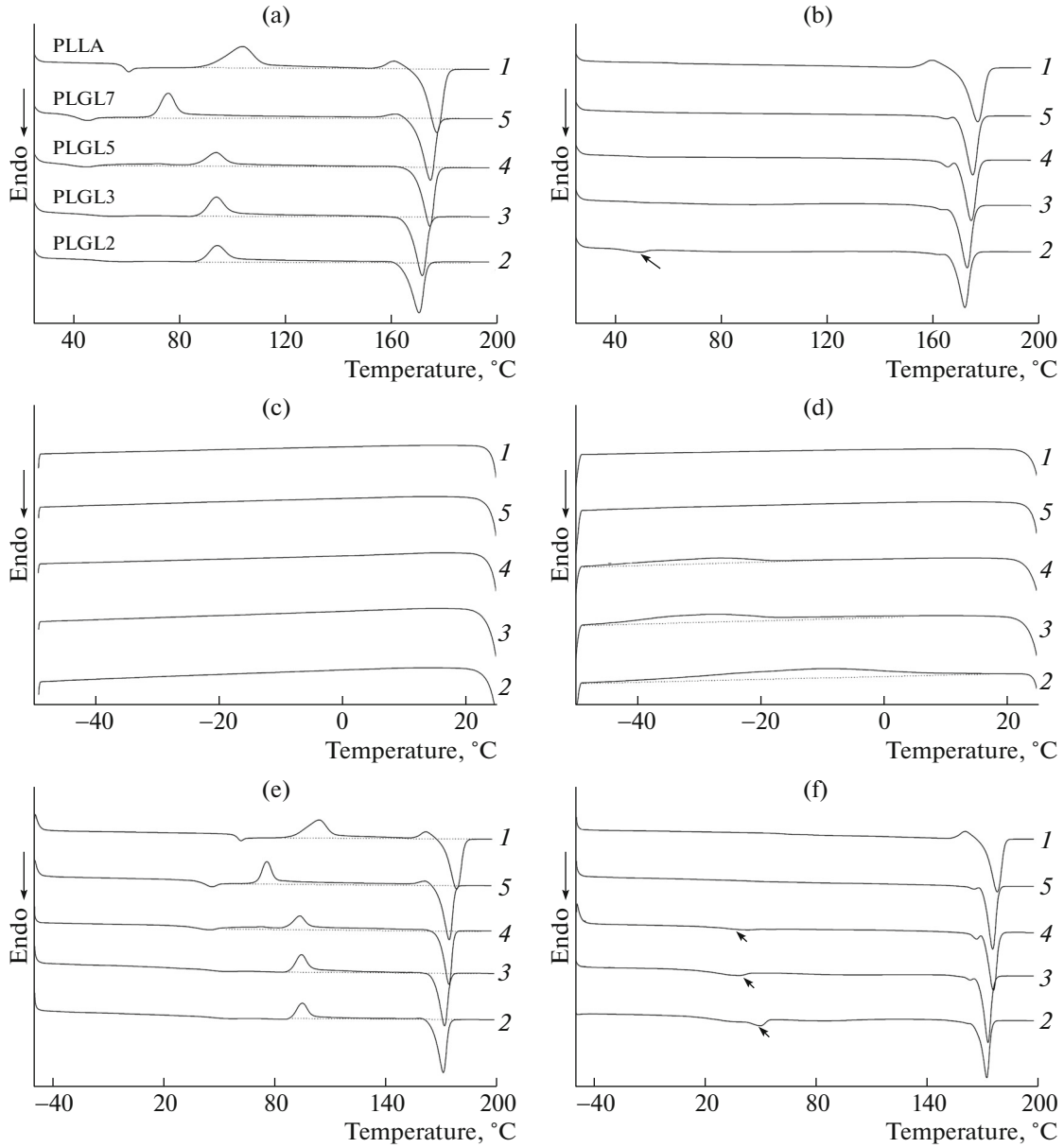

Fig. 2. DSC heating scans of (a) amorphous and (b) crystalline (*1*) PLLA and PLLA–PEG–PLLA copolymers: (*2*) PLGL 2, (*3*) PLGL 3, (*4*) PLGL 5, (*5*) PLGL 7 form 25 to 200°C; DSC cooling scans of (c) amorphous and (d) crystalline PLLA and PLLA–PEG–PLLA copolymers form 25 to −50°C; DSC second heating scans of (e) amorphous and (f) crystalline PLLA and PLLA–PEG–PLLA copolymers form −50 to 200°C. The dot line is baseline.

for neat PLLA and PLGL7 over the temperature range of 30~120°C. However, with the increase of PEG, small endothermic peaks due to the T_ms of PEG blocks were observed for PLGL5 ~ PLGL2. Meanwhile, a recrystallization peak and a clear melting peak were observed for all copolymers. Similar to amorphous samples, the melting peak shifted to lower temperatures with decreasing PLLA chain length, which suggested a decrease in T_m. The recrystallization peak became smaller with higher PEG percentage. As shown in Table 2, the X_c of neat PLLA was 49.2% and the value increased with the molecular weight of PLLA blocks decreasing. The X_c of PLLA block in crystallized PLGL2 reached 65% and further higher than that of amorphous PLGL2. This indicates that all PLLA block were in highly crystalline state in crystallized samples.

However, as PEG increased to more than 14.8 wt % (Table 1), broad but unobvious melting and crystallization peaks attributed to PEG block can be observed for PLGL5, PLGL3 and PLGL2 after enlarging the heating curves. The T_m, ΔH_m and X_c of PEG blocks are listed in Table 2. It can be seen that the X_c of PEG

Table 2. Thermal properties of PLLA and PLGL copolymers

Samples		PEG block			PLLA block				
		T_m[a], °C	ΔH_m[a], J/g	X_c, %	T_{cc}[a], °C	ΔH_{cc}[a], J/g	T_m[a], °C	ΔH_m[a], J/g	X_c, %
Amorphous	PLLA	–	–	–	104.1	42.3	177.2	44.1	1.9
	PLGL7	–	–	–	75.5	32.1	174.8	33.6	1.9
	PLGL5	–	–	–	94.0	31.4	174.4	38.8	9.3
	PLGL3	–	–	–	94.1	32.2	171.7	39.5	10.0
	PLGL2	–	–	–	94.5	28.8	170.5	38.8	14.6
Crystalline	PLLA	–	–	–	–	–	177.1	45.8	49.2
	PLGL7	–	–	–	–	–	175.1	45.1	54.8
	PLGL5	53.3	0.3	1.0	–	–	174.5	47.8	60.3
	PLGL3	51.7	0.5	1.1	–	–	172.9	44.0	60.2
	PLGL2	53.5	2.0	3.7	–	–	171.6	44.6	65.0

[a]Determined by DSC heating scan (25→200°C); ΔH_m and ΔH_{cc} were normalized with weight percentage of PLLA (or PEG).

Table 3. Thermal properties of PEG blocks in PLGL copolymers

Samples		T_g[a], °C	T_c[b], °C	ΔH_c[b], J/g	T_m[c], °C	ΔH_m[c], J/g	X_c, %
Amorphous	PLLA	59.5	–	–	–	–	–
	PLGL7	43.0	–	–	–	–	–
	PLGL5	39.3	–	–	–	–	–
	PLGL3	28.4	–	–	–	–	–
	PLGL2	17.1	–	–	–	–	–
Crystalline	PLLA	62.1	–	–	–	–	–
	PLGL7	45.2	−34.5	0.2	36.5	0.3	1.3
	PLGL5	34.6	−27.8	2.6	41.9	6.5	21.1
	PLGL3	30.5	−28.9	4.9	36.6	10.5	23.6
	PLGL2	21.6	−10.3	9.9	49.4	17.8	32.7

[a] Determined by MDSC.
[b] Determined by DSC cooling scan (25→−50°C).
[c] Determined by following heating scan (−50→200°C); ΔH_m and ΔH_{cc} were normalized with weight percentage of PEG.

blocks in those three samples were in range of 1.0 ~ 3.7% and was kept increasing with increase of PEG block. This result indicated that like amorphous samples, most of PEG blocks in the crystalline PLGL samples were also in amorphous state.

From above analysis, no obvious crystallized PEG was observed in both amorphous and crystallized samples as shown in Figs. 2a, 2b. This result might suggest that the PEG blocks in both amorphous and crystalline samples were in the amorphous state. To further investigate the crystalline state of PEG blocks in copolymers, all samples were firstly cooled to −50°C and then heated to 200°C at 10 grad/min.

Figures 2c–2f depict the cooling curves from 25 to −50°C and the following heating scan from −50 to 200°C, respectively. The T_c, ΔH_c and X_c of PEG blocks obtained from the cooling process, the T_m and ΔH_m of PEG obtained from heating curves were summarized Table 3.

Figures 2c, 2d present the cooling curves of amorphous and crystalline samples, respectively. It can be seen that all amorphous samples have smooth curves without any exothermic peaks. Meanwhile, as presents in Fig. 2e, also no distinct endothermic peaks correspond to the melting of PEG were observed for amorphous samples when heating from −50 to 200°C.

For neat PLLA, a typical T_g appeared at about 60°C, following by a with a small enthalpy relaxation peak. The T_gs of PLGL7 and PLGL5 slightly shifted to lower temperature and similar enthalpy relaxation peak also was observed for those two samples. With all of these phenomena together, suggesting that PEG blocks were in amorphous state and dispersed homogeneously in this miscible copolymer system. The

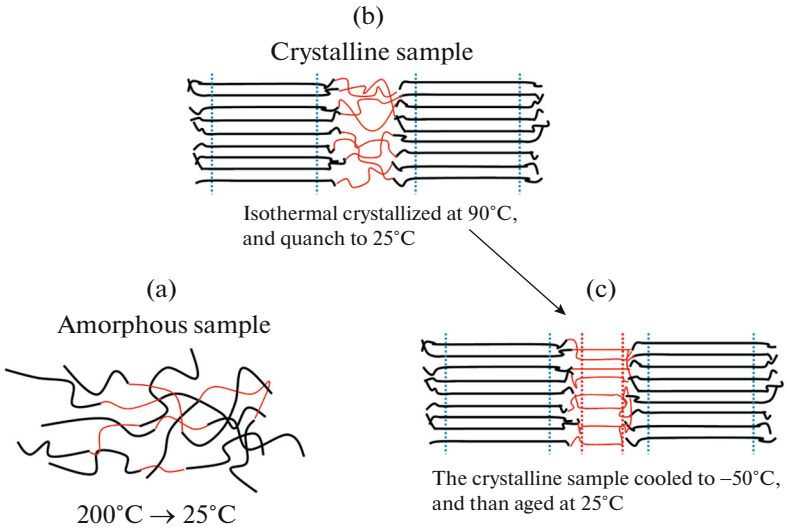

Fig. 3. (Color online) Schematic diagram of amorphous and crystalline samples were treated by hot pressing.

PEG chain cannot aggregate and even cannot crystallization at low temperature in this homogenous system.

For crystalline samples, there are still no obvious peaks appeared for PLLA as shown in Fig. 2d during cooling process. In the cause of PLGL7, the exothermic peak due to the crystallization of PEG blocks can be observed when enlarged the cooling curve. With more PEG in the PLGL triblock copolymers, small exothermic peaks can be distinct observed for PLGL5 and become broader for PLGL3 and PLGL2, which indicated that the PEG blocks in these copolymers could only crystallize at the temperature below room temperature.

When firstly cooling from 25 to −50°C, the original aggregated liquid state PEG chains started to crystallize. Thus the crystallization appeared for cooling curves of PLGL films. As shown in Table 3, the X_c of PLGL7 was only 1.3%. The X_c increased with increasing PEG. For PLGL 5, the X_c value reached to 21.1%. The X_c of PLGL2 increased to 32.7%, almost 25 times of that of PLGL7. Meanwhile, obvious melting peaks of PEG blocks appeared in PLGL5, PLGL3 and PLGL2 in Fig. 2f. Consider both cooling and heating curves, those results well proved that the amorphous PEG block was originally alternating arranged with the orderly crystallized PLLA block in crystallized samples.

Once the PLLA blocks started to arrange orderly and formed lattice, the PEG as the middle chain also was forced to aggregate. Although the crystallized samples were cooling to 25°C after melting at 200°C during hot-press process, the middle PEG chain was in an amorphous state, almost no PEG crystallite existed in this situation. Thus no obvious diffraction peak attributed to the crystals of PEG was observed for crystallized copolymers in WAXD spectrum. And this result also well explained why there are almost no obvious melting peaks in DSC curves when the crystalline PLGL copolymers were firstly heating from 25 to 200°C (Fig. 2b).

On basis of the aforementioned results, the crystallization mechanism of PLLA and PEG blocks in amorphous and crystallized samples are proposed, as illustrated in Fig. 3. As confirmed by WAXD, no obvious crystallization peaks were observed for amorphous films. As presents in Fig. 3a when the copolymer melting at 200°C during hot-press, then the film was quickly cooled to room temperature (about 25°C), the molecular chains were intertwined and disorderly arranged. PLLA blocks cannot orderly aggregate and crystallization, as well as PEG blocks.

However, in the case of films kept at 90°C for fully crystallizing, the PLLA blocks quickly crystallized and ordered arranged. And the middle PEG blocks were forced to aggregate, but still kept at amorphous states as shown in Fig. 3b [72]. That well according with WAXD spectrum and clearly explained why no distinct melting and crystallization peaks of PEG for crystallized samples when firstly scanning from 25 to 200°C. When the crystallized sample was cooled to −50°C in DSC test, the original amorphous PEG middle blocks started to crystallization as shown in Fig. 3c. Thus the crystallization peaks appeared in the DSC cooling curves of crystallized PLGL films, then obvious melting peaks appeared during heating from −50 to 200°C.

Isothermal Crystallization Behavior

Figure 4 presents the DSC thermograms of isothermal crystallization of samples at 80, 90 and 100°C, respectively. It can be seen from Fig. 4a, the crystalli-

zation of PLLA is very slow, and it takes more than one hour for a completely crystallization at 80°C. However, all PLGL triblock copolymers are completely crystallized in few minutes at the same condition. That is to say the presence of PEG block accelerated the crystallization rate of PLLA. In addition, from PLGL7 to PLGL3, the crystallization time decreased with increasing PEG block content. There are two mainly reasons accounting for this phenomenon: (1) it has been reported that the molecular weight significantly affects the crystallization kinetics the crystallization of PLLA, and the crystallization rate reduces greatly with the molecular weight increasing. The molecular weight of PLLA blocks in PLGL copolymers are decreasing, thus lead a more rapidly crystallization rate of PLLA and a shorter crystallization time. (2) the longer PEG chain length in the middle segment permits a higher mobility of the adjacent PLLA molecular chain and enhance the crystallization of PLLA chains [73]. However, it should be noticed that the PLGL3 shows shortest crystallization time rather than PLGL2 in range of 80 ~ 100°C. One possible reason is that when the crystallization of PLLA starting, the PEG blocks is in an amorphous state. The existence of large amount of PEG block has a dilution effect on the copolymer system and leads a dispersion of PLLA block. Thus decreases the crystallization rate of PLLA in PLGL2 copolymer [74].

As shown in Fig. 4b, both neat PLLA and copolymers show a more rapidly crystallization rate at 90°C. For neat PLLA, the crystallization time is only about 1/5 of that of 80°C. Nevertheless, it still take a relative longer time for a fully crystallize process of the neat PLLA when compared with copolymers. At 100°C, the copolymers are fully crystallized in less than 4 min and show more obvious crystallize peaks as shown in Fig. 4c. Meanwhile, the neat PLLA also completely crystallized and the crystallization time decreased to less than 10 minutes. Clearly, the crystallization rates of PLGL copolymers containing middle PEG blocks are much higher than that of the pure polymer, confirming the PEG middle block segment greatly enhances effectively the crystallization of the PLLA.

POM Analysis

POM was used to monitor the growth and size of the spherulites. Figure 5 shows the spherulitic morphologies of PLLA and PGLA triblock copolymers with different PEG content. At 100°C, it can be seen that small spherulites were densely arranged for neat PLLA. After insertion of PEG blocks, the density of nuclei was decreased and the spherulites size of PLGL7 was larger. With further increasing PEG content, the density of nuclei further decreased and the spherulites of PLGL7 and PLGL5 show a rotating growing from a center. However, the stripes of PLGL3 and PLGL2 spherulites are obscure.

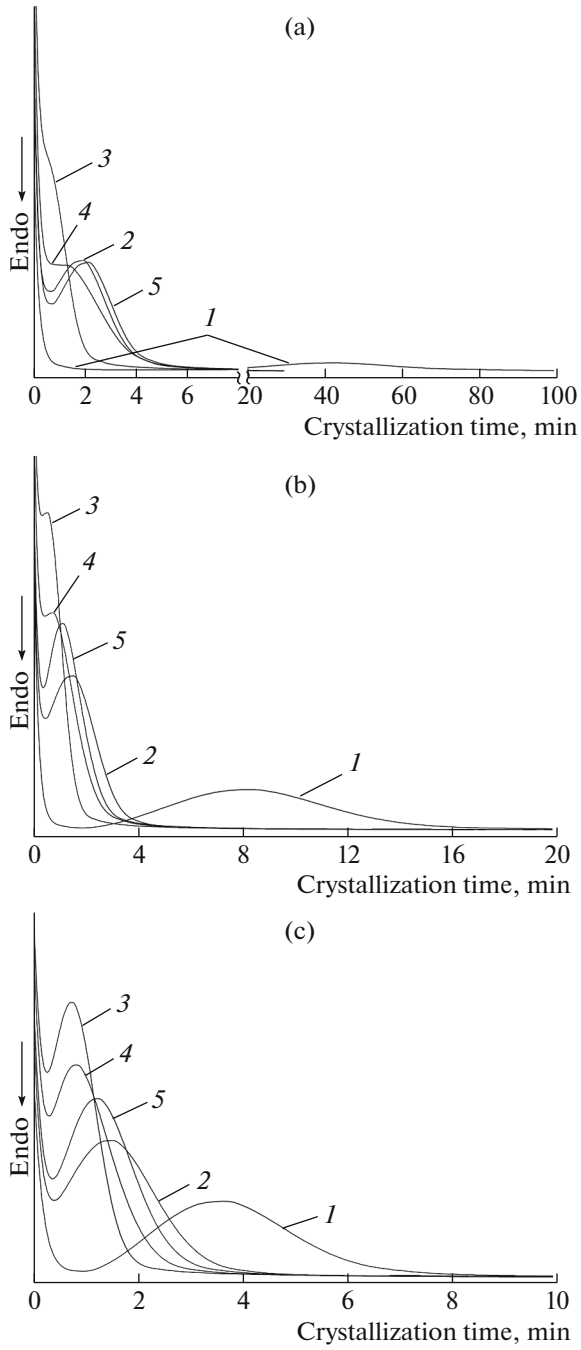

Fig. 4. DSC heating curves of (*1*) PLLA and PLLA–PEG–PLLA copolymers: (*2*) PLGL 2, (*3*) PLGL 3, (*4*) PLGL 5, (*5*) PLGL 7 recorded in (a) isothermal melt crystallization at 80°C and (b) isothermally melt-crystallized at 90°C and (c) isothermally melt-crystallized at 100°C.

The spherulites radius growth rate G of samples were also calculated from micrographs of isothermal crystallization at 100~130°C and listed in Fig. 6, the G values of all copolymers decreased with increasing temperature at tested condition. The neat PLLA shows a slow spherulites radius growth rate and small-

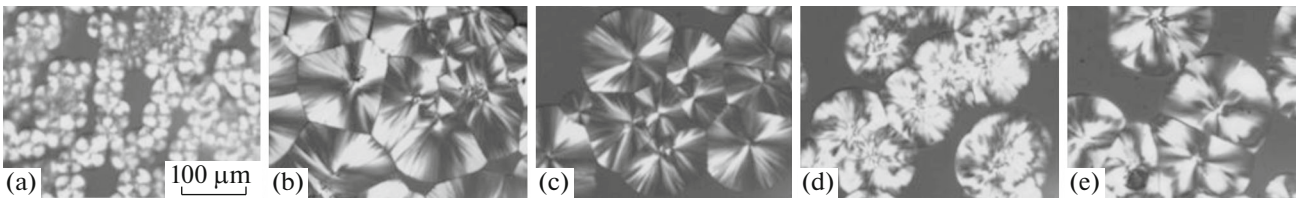

Fig. 5. Optical micrographs of neat PLLA and PLGL copolymers isothermally melt-crystallized at 100°C: (a) neat PLLA, (b) PLGL7, (c) PLGL5, (d) PLGL3, and (e) PLGL2.

est *G* value. The second-slowest spherulites radius growth rate at the same condition was assigned to PLGL2 copolymer. The PLGL7 owns *G* value higher than PLGL2 and lower than PLGL5. The PLGL3 has the most rapid spherulites radius growth rate among all samples, and this result is very consistent with DSC results in Fig. 4.

Tensile Behavior Analysis

Exemplary stress-strain dependencies for the materials studied are plotted in Fig. 7 and average values of elongation at break, yield stress and Young's modulus are listed in Table 4. As seen in Fig. 7a, neat amorphous PLLA yield at about deformation of 7% and the stress above 35 MPa and exhibited poor drawability as reported [46]. The existence of PEG blocks caused a decrease of the yield stress and an increased elongation at break in all amorphous copolymers. As shown in Table 4, the average elongation at break of PLGL7 reached more than 280% and that is almost 40 times of neat PLLA. The average elongation at break of PLGL2 was as high as 530%. The elongation at break of PLGL copolymers increased with increasing PEG contents, while the yield stress decreased with increase of PEG contents, indicating

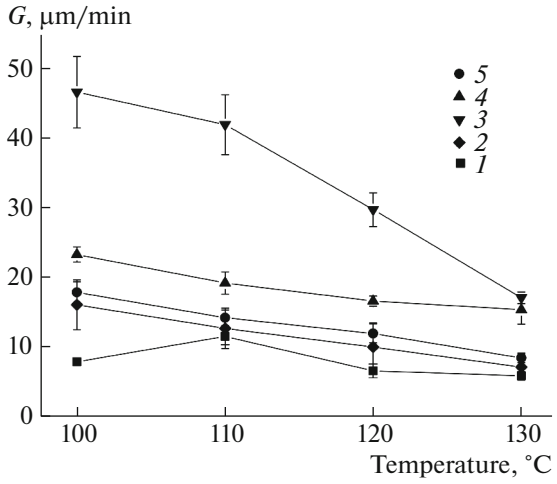

Fig. 6. Spherulites radius growth rate of (*1*) neat PLLA and PLGL copolymers: (*2*) PLGL 2, (*3*) PLGL 3, (*4*) PLGL 5, (*5*) PLGL 7 measured in melt-crystallization at 80~130°C.

that PEG blocks greatly increased the toughness of PLLA.

In the case of crystallized samples, as shown in Fig. 7b, neat PLLA shows a brittle fracture before yield and the fracture strain was only about 2%. For copolymers, the PEG blocks still caused a lower stress of polymers. The PLGL7 has highest value of elongation at break about 120% and the elongation decreased with increasing PEG segments. The elongation at break decreased to about 30% for PLGL2, the value still was about 15 times of neat PLLA with the same treatment. However, a completely different with amorphous samples is only a typical yield point appeared for PLGL7, and no obvious yield points were observed in other copolymers with increasing content of PEG segments.

The mechanical properties of PLLA are dependent on the morphology and the amount of crystalline fraction developed during different treatments. This total different behavior can be explained in terms of finally different morphologies [75]. When copolymers are in amorphous state, both PEG and PLLA blocks appeared a good compatibility and their chain has quite good mobility, especially with relative longer PEG blocks. The chains dispersion and the copolymer were homogeneous. Thus can avoid stress concentration and lead a more and more good drawability of copolymer [76].

For crystallized PLGL copolymers, on one hand the brittleness was increased by the crystallization; On the other hand, the phase separation may occur with higher PEG content, as previously shown in Fig. 5, fewer and larger spherules formed and the spherulite's morphologies changed with increasing PEG blocks. The decrease of crystal nucleus and structural change of spherulite's boundaries may promote stress concentrations, thus finally lead a decrease in elongation with longer PEG blocks for copolymers [75–79].

Young's modulus also is an important physical quantity for materials resist deformation ability. As seen in Table 4, the amorphous neat PLLA has a Young's modulus above 698 MPa, which indicates a high rigidity of material. However, with incorporation of PEG blocks, the Young's modulus of PLGL7 decreased to almost 3/5 of neat PLLA. And the Young's modulus of copolymers kept decreasing with increase of PEG content. The modulus of PLGL2 was

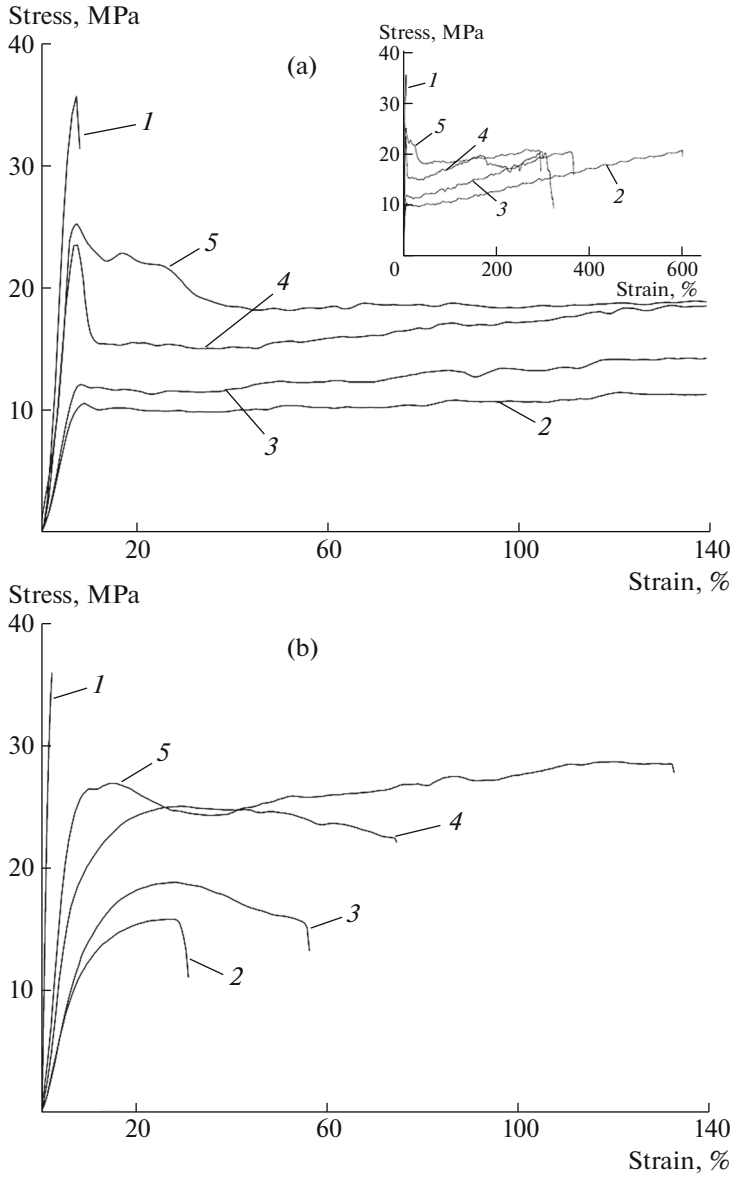

Fig. 7. Strain-stress curves of (*1*) PLLA and PLGL copolymers: (*2*) PLGL 2, (*3*) PLGL 3, (*4*) PLGL 5, (*5*) PLGL 7: (a) amorphous and (b) crystallized samples.

only about 164 MPa and that was only about 1/5 of neat PLLA. It can be seen from Table 4, the Young's modulus of copolymers in crystallized samples shows the similar tendency with amorphous ones.

In general, the Young's modulus of the crystallized polymer is higher than amorphous ones. However, except the neat PLLA, the modulus of crystalline samples was slightly decreased when compared with amorphous samples. Consider the WAXD result shown in Fig. 1b, no crystallization peaks of PEG were observed for all copolymers, indicating the molten state of PEG in crystallized samples. The existence of flexibility PEG segments eventually leads a lower Young's modulus of the crystallized PLGL copolymers. Consider the whole result, although the strength of material decreased, the toughness of material was well improved with the presence of PEG blocks for both amorphous and crystallized samples.

Morphology of Fracture Surface

The SEM micrographs can further reveal the fracture characteristics of samples. Figure 8 shows SEM micrographs of fracture surface of both amorphous and crystallized neat PLLA and PLGL copolymers. Figures 8a–8e was the micrographs of fracture surface of amorphous samples and the Figs. 8f–8j were the crystallized samples.

Table 4. Results of tensile tests for both amorphous and crystallized PLLA and PLGL copolymers

Treatment	Samples	Young' modulus, MPa	Yield strength, MPa	Elongation at break, %
Amorphous samples	PLLA	698.1 ± 32.7	30.4 ± 7.4	6.4 ± 2.6
	PLGL7	468.6 ± 17.3	28.1 ± 4.0	283.3 ± 23.2
	PLGL5	376.6 ± 28.3	24.5 ± 6.2	348.0 ± 33.9
	PLGL3	187.4 ± 8.1	15.9 ± 5.4	381.0 ± 21.2
	PLGL2	163.1 ± 17.5	10.6 ± 2.4	530.0 ± 98.9
Crystallized samples	PLLA	1929.8 ± 86.3	30.4 ± 6.7	2.2 ± 0.4
	PLGL7	360.9 ± 14.9	26.3 ± 1.5	118.1 ± 20.6
	PLGL5	304.9 ± 10.2	25.8 ± 1.1	91.1 ± 23.4
	PLGL3	180.5 ± 1.3	15.8 ± 3.3	46.6 ± 13.6
	PLGL2	164.3 ± 6.2	15.7 ± 2.3	35.6 ± 6.6

It can be seen from Fig. 8a that neat PLLA has a quiet uniform and smooth and fracture surface, which is related with its brittleness. In the case of PLGL7, little amount of plastic deformation were observed on a relative rough fracture surface. With further increasing PEG content, the surface becomes rougher and large amount of plastically deformed walls were distinguishable on fracture surfaces of other PLGL copolymers. In addition, the boundary of PLGL5, PLGL3 and PLGL 2 become visible with similar original thickness at the same magnification, also indicating a thinner film and better tensile property of samples.

In the case of crystallized samples, the neat PLLA showed a much more homogeneous typical brittleness fracture surface. After the insertion of PEG blocks, obvious patterns of hollows surrounded by plastically deformed walls were observed for PLGL7. Further increasing the PEG content, on the fracture surfaces of crystalline PLGL5, PLGL3 and PLGL2 copolymers, the plastic deformation walls were more independent. Meanwhile, the drawn deformed walls decreased with increasing PEG contents, which suggesting a decrease in anti-deformation ability and the copolymer showed ductile failure. The SEM results were well according with the tensile result before.

DMA Analysis

Figure 9 depicts the dynamic mechanical spectra of both amorphous and crystalline samples with different PEG content. From Fig. 9a, among all the amorphous samples, the PLLA has a higher storage modulus than those of the amorphous PLGL copolymers, and its storage modulus shows a slowly decrease in range of −100 to 50°C, then a sharply decrease occurred in the temperature range of 50 to 80°C.

It could be seen for the amorphous PLGL samples that the storage modulus varied very little in the first section of the curve with temperature increasing from −100 to 25°C. Then a sharp decrease was observed, which attributed to the change in the segmental mobility related to the glass transition. The value of storage modulus increased drastically again around 70–110°C because of the cold crystallization of the

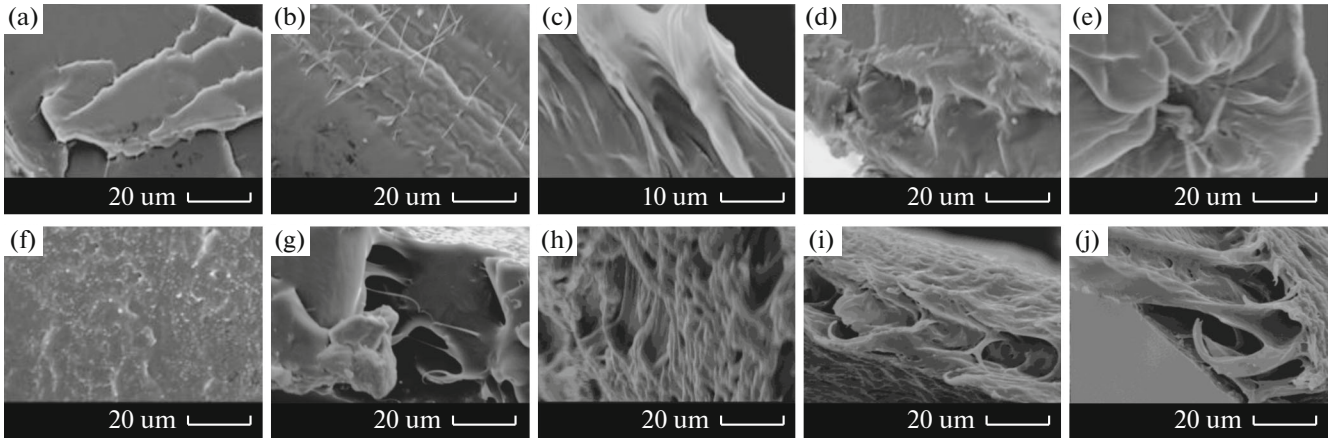

Fig. 8. SEM micrographs of fracture surfaces of tensile specimens: (a) neat PLLA, (b) PLGL7, (c) PLGL5, (d) PLGL3, (e) PLGL2, room temperature treatment, and (f) neat PLLA, (g) PLGL7, (h) PLGL5, (i) PLGL3, (j) PLGL2, 90°C treatment.

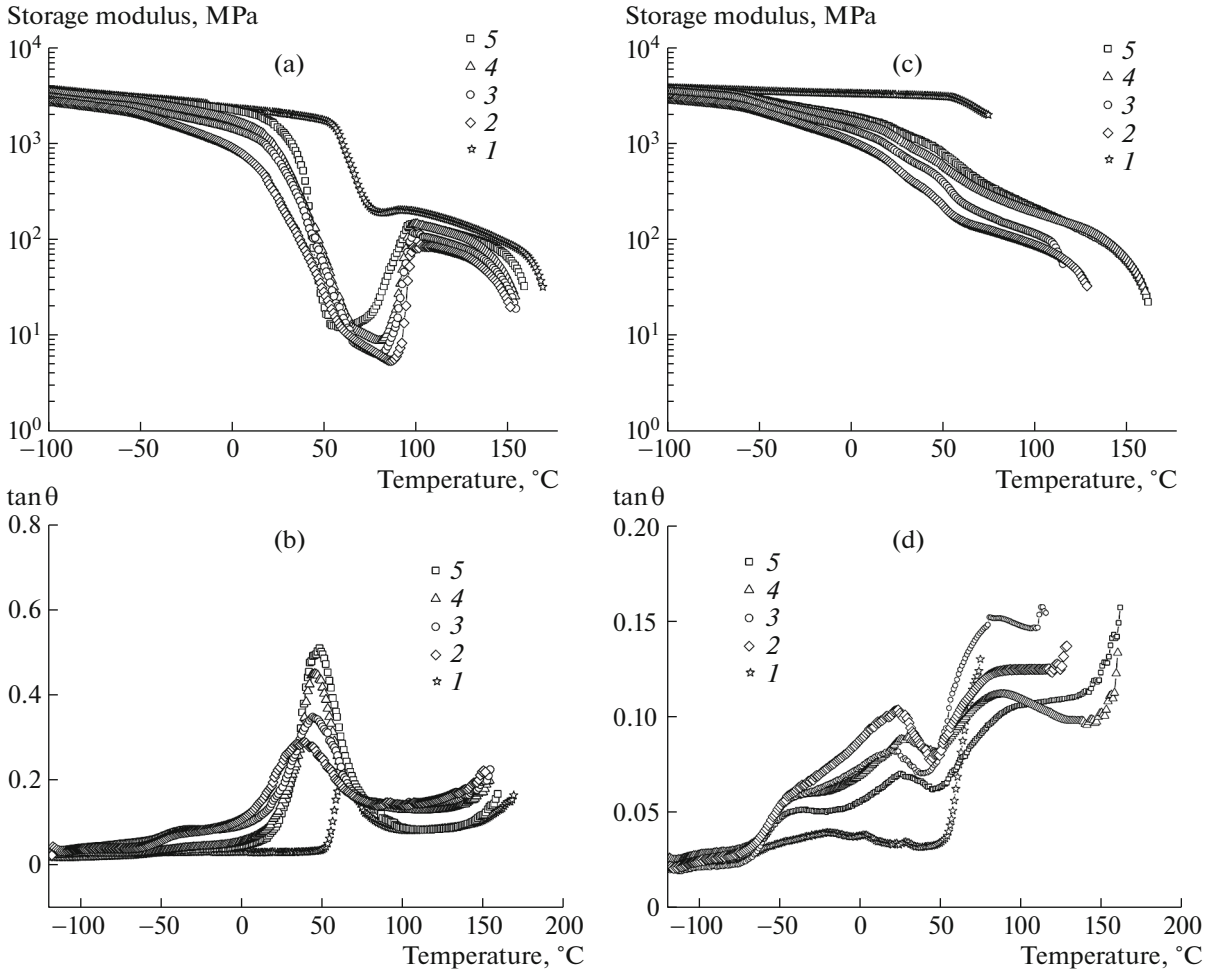

Fig. 9. DMTA curves of (*1*) PLLA and PLGL triblock copolymers: (*2*) PLGL 2, (*3*) PLGL 3, (*4*) PLGL 5, (*5*) PLGL 7: (a) storage modulus of amorphous samples, (b) tan θ of amorphous samples, (c) storage modulus of crystallized samples, and (d) tan θ of crystallized samples.

PLLA blocks. However, the value of storage modulus decreased rapidly with increasing PEG content in the PLGL copolymers.

Figure 9b displays the loss tangent (tan θ) of amorphous PLLA and PLGL triblock copolymers. A sharp peak of tan θ appeared at about 6°C, which assigned to the α-transition of the neat PLLA around its T_g [80]. This can well explain the sharply decrease of storage modulus of PLLA between 50 and 80°C. For amorphous PLGL copolymers, very small peaks can be observed at about −60°C due to the α-transition of PEG blocks [35]. That is why the storage modulus values of copolymers showed a slowly decrease at about −50°C. The value of the tan θ on the α-transition peak top of PLGL7 was very higher than those of neat PLLA, and this peak decreased with increase of PEG content. The T_g, determined as the temperature corresponding to the maximum of tan θ in the α-transition, decreased with the PEG content, suggesting relative good compatibility between both PEG and PLLA blocks. This was basically in accordance with the DSC results.

Figure 9c given the storage modulus of crystallized samples. Similarly, the neat PLLA maintain a quiet stable storage modulus until its glass transition temperature and fractured around its melt temperature. Nevertheless, the change of storage modulus of copolymers was quite differently than amorphous ones. As shown in Fig. 9d, the storage modulus values of copolymers almost unchanged in the temperature range of −100 to −50°C, then a decrease began until the fracture of samples at above 120°C. This is to say the presence of PEG blocks greatly improved the flexibility of PLLA.

In the curves of tan θ, peaks assigned to T_g of PEG and PLLA were observed at about −60 and 70°C for copolymers, respectively, suggesting phase separation occurred in the PLGL copolymer system. It should be noticed that a small peak also appeared around 30°C for copolymers and the peak become sharper with

increasing PEG content. Consider the previous DSC results, it may due to the melting of PEG. Thus lead a relative rapidly decrease of storage modulus of copolymers at −50 ~ 25°C compared with amorphous samples. The results proved again that the PEG blocks can confine crystallize between PLLA crystals lamellar as shown in Fig. 3.

CONCLUSIONS

High molecular weight PLLA–PEG–PLLA triblock copolymers with different lengths of PLLA blocks were synthesized by ring opening polymerization in this work. Then, polymer films were prepared by hot pressing and obtained amorphous and crystallized samples through different temperature treatment. PLLA and PEG blocks exhibited good miscibility in the amorphous PLGL samples, while the phase separation occurred in the crystalline ones. The WAXD and DSC results showed that the PEG blocks almost adopt the amorphous state in both amorphous and crystalline PLGL. Since the PEG blocks were homogeneously dispersed in the amorphous PLGL matrix, two phase exhibited good miscibility, and the maximum fracture strain reached about 600%. The flexible PEG blocks also increase the toughness of the PLLA. However, the fracture strain of crystalline PLGL samples lower than that of the amorphous samples due to phase separation and liquid state of PEG. In addition, with the incorporation of PEG middle blocks in the PLGL copolymers, the spherulites growth rate was greatly increased and the crystallization time of copolymers shorten to only less than 6 min in temperature range of 80~100°C. For further use in food packaging, the soft PEG segment improve the processability and toughness of PLLA, and since the PEG was covalently incorporated in the PLLA main chain, avoid the migration of PEG from the plastic result in lower the mechanical properties of packaging film and the contamination of foods.

ACKNOWLEDGMENTS

The authors thank the National Natural Science Foundation of China (no. 21564012) and Scientific and Technological Innovation Guide Award Project of Inner Mongolia Autonomous Region (2016).

REFERENCES

1. C. H. Hong, H. K. Si, J. Y. Seo, and D. S. Han, ISRN Polym. Sci. **2012**, 938261 (2012).
2. O. Cheerarot and Y. Baimark, J. Chem. **2015**, 206123 (2015).
3. J. Ren, H. Hong, J. Song, and T. Ren, J. Appl. Polym. Sci. **98**, 1884 (2005).
4. S. Lee, Z. Zhang, and S. Feng, Biomaterials **28**, 2041 (2007).
5. M. Prabaharan, J. J. Grailer, S. Pilla, D. A. Steeber, and S. Gong, Macromol. Biosci. **9**, 515 (2009).
6. H. He, J. Yu, J. Cao, L. E, D. Wang, H. Zhang, and H. Liu, J. Biomater. Sci., Polym. Ed. **22**, 179 (2011).
7. M. W. Yuan, Y. Y. Qin, J. Y. Yang, Y. Wu, M. L. Yuan, and H. L. Li, Arzneim. Forsch. **9**, 231(1959).
8. D. V. Plackett, V. K. Holm, P. Johansen, S. Ndoni, P. V. Nielsen, T. Sipilainen-Malm, S. Anders, and V. Steven, Packag. Technol. Sci. **19**, 1 (2006).
9. A. Martínez-Abad, J. M. Lagarón, and M. J. Ocio, Food Control **43**, 238 (2014).
10. P. Pan, Z. Bo, W. Kai, S. Serizawa, M. Iji, and Y. Inoue, J. Appl. Polym. Sci. **105,** 1511 (2007).
11. G. Perego, G. D. Cella, and C. Bastioli, J. Appl. Polym. Sci. **59**, 37 (1996).
12. Y. Li and H. Shimizu, Eur. Polym. J. **45**, 738 (2009).
13. J. B. Zeng, Y. D. Li, Y. S. He, S. L. Li, and Y. Z. Wang, Ind. Eng. Chem. Res. **50**, 6124 (2011).
14. X. Fan, J. M. Ruan, Q. Y. Chen, J. Chen, Z. C. Zhou, and J. P. Zou, J. Macromol. Sci., Part B: Phys. **50**, 493 (2011).
15. N. Eawwiboonthanakit, M. Jaafar, Z. A. A. Hamid, M. Todo, and B. Lila, Adv. Mater. Res. **1024**, 179 (2014).
16. M. Todo and T. J. Takayama, Mater. Sci. **42**, 4712 (2007).
17. L. Jiang, M. P. Wolcott, and J. Zhang, Biomacromolecules **7**, 199 (2006).
18. *The Technology of Plasticizers,* Ed. by J. K. Sears and J. R. Darby (Wiley and Sons, New York, 1982).
19. O. Martin and L. Averous, Polymer **42**, 6209 (2001).
20. E. Piorkowska, Z. Kulinski, A. Galeski, and R. Masirek, Polymer **47**, 7178 (2006).
21. Z. Kulinski, E. Piorkowska, K. Gadzinowska, and M. Stasiak, Biomacromolecules **7**, 2128 (2006).
22. A. J. Nijenhuis, E. Colstee, D. W. Grijpma, and A. J. Pennings, Polymer **37**, 5849 (1996).
23. S. Jacobsen and H. G. Fritz, Polym. Eng. Sci. **39**, 1303 (1999).
24. O. Martin and L. Avérous, Polymer **42**, 6209 (2001).
25. M. Baiardo, G. Frisoni, M. Scandola, M. Rimelen, D. Lips, K. Ruffieux, and E. Wintermantel, J. Appl. Polym. Sci. **90**, 1731 (2003).
26. Y. Hu, M. Rogunova, V. Topolkaraev, A. Hiltner, and E. Baer, Polymer **44**, 5701 (2003).
27. Z. Kulinski and E. Piorkowska, Polymer **46**, 10290 (2005).
28. Z. Jia, J. Tan, C. Han, Y. Yang, and L. Dong, J. Appl. Polym. Sci. **114**, 1105 (2009).
29. H. Xiao, F. Liu, T. Jiang, and J. T. Yeh, J. Appl. Polym. Sci. **117**, 2980 (2010).
30. O. Martin and L. Avérous, Polymer **42**, 6209 (2001).
31. V. S. G. Silverajah, N. A. Ibrahim, M. Z. W. Y. Wan, H. A. Hassan, and C. B. Woei, Int. J. Mol. Sci. **13**, 5878 (2012).
32. X. Zhang, J. Sun, S. Fang, X. Han, Y. Li, and C. Zhang, J. Appl. Polym. Sci. **122**, 296 (2011).
33. S. Saadatmand, U. Edlund, and A. C. Albertsson, Polymer **52**, 4648 (2011).

34. T. Michinobu, M. Bito, M. Tanimura, Y. Katayama, E. Masai, M. Nakamura, Y. Otsuka, S. Ohara, and K. Shigehara, Polym. J. **41**, 843 (2009).
35. W. Kai, L. Zhao, B. Zhu, and Y. Inoue, Macromol. Rapid. Commun. **27**, 109 (2006).
36. J. Ding, S. C. Chen, X. L. Wang, and Y. Z.Wang, Ind. Eng. Chem. Res. **48**, 788 (2008).
37. N. Tudorachi and R. Lipsa, J. Appl. Polym. Sci. **122**, 1109 (2011).
38. C. Ba, J. Yang, Q. Hao, X. Liu, and A. Cao, Biomacromolecules, **4**, 1827 (2003).
39. Y. Huang, P. Pan, G. Shan, and Y. Bao, RSC Adv. **4**, 47965 (2014).
40. S. C. Schmidt and M. A. Hillmyer, J. Polym. Sci., Part B: Polym. Phys. **39**, 300(2001).
41. O. Martin, E. Schwach, L. Avérous, and Y. Couturier, Starch/Staerke **53**, 372 (2001).
42. C. A. Mitchel and R. Krishnamoorti, Macromolecules **40**, 1538 (2007).
43. N. Ljungberg and B. Wesslén, Biomacromolecules **6**, 1789 (2005).
44. Y. Li, X. Li, F. Xiang, T. Huang, Y. Wang, J. Wu, and Z. W. Zhou, Polym. Adv. Technol. **22**, 1959 (2011).
45. N. Kawamoto, A. Sakai, T. Horikoshi, T. Urushihara, and E. Tobita, J. Appl. Polym. Sci. **103**, 198 (2007).
46. T. Dong, Z. Yu, J. Wu, Z. Zhao, X. Yun, Y. Wang, Y. Jin, and J. Yang, Polym. Sci., Ser. A **57**, 738 (2015).
47. P. Pan, Z. Liang, B. Zhu, T. Dong, and Y. Inoue, Macromolecules **42**, 3374 (2009).
48. J. Yang, Y. Qin, M. Yuan, X. Jing, J. Cao, W. Yan, and M. Yuan, Int. J. Biol. Macromol. **6**, 411(2013).
49. T. Ke and X. Sun, J. Appl. Polym. Sci. **89**, 1203 (2003).
50. Y. H. Cai, J. Chem. **9**, 1569 (2012).
51. L. Han, P. Pan, G. Shan, and Y. Bao, Polymer **63**, 144 (2015).
52. K. S. Anderson and M. A. Hillmyer, Polymer **47**, 2030 (2006).
53. X. F. Wei, R. Y. Bao, Z. Q. Cao, W. Yang, B. H. Xie, and M. B. Yang, Macromolecules **47**, 1439(2014).
54. J. Sun, H. Yu, X. Zhuang, X. Chen, and X. Jing, J. Phys. Chem. B **115**, 2864 (2011).
55. H. Urayama, T. Kanamori, K. Fukushima, and Y. Kimura, Polymer **44**, 5635 (2003).
56. G. Jimenez, N. Ogata, H. Kawai, and T. Ogihara, J. Appl. Polym. Sci. **35**, 389 (1997).
57. Z. Ru, Y. Wang, K. Wang, G. Zheng, L. Qian, and C. Shen, Polym. Bull. **70**, 195 (2013).
58. N. Kawamoto, A. Sakai, T. Horikoshi, T. Urushihara, and E. Tobita, J. Appl. Polym. Sci. **103**, 198(2007).
59. Y. Li, Y. Wang, L. Liu, L. Han, F. Xiang, and Z. Zhou, J. Polym. Sci., Part B: Polym. Phys. **47**, 326 (2008).
60. J. Y. Nam, M. Okamoto, H. Okamoto, M. Nakano, A. Usuki, and M. Matsuda, Polymer **47**, 1340 (2006).
61. Y. Li, H. Wu, Y. Wang, L. Li, H. Liang, J. Wu, and F. Xiang, J. Polym. Sci., Part B: Polym. Phys. **48**, 520 (2010).
62. M. A. Ramos and J. P. V. Matheu, Polym. Compos. **9**, 105(1988).
63. H. Xiao, L. Yang, X. Ren, T. Jiang, and J. T. Yeh, Polym. Compos. **31**, 2057 (2010).
64. L. Feng, X. Bian, Y. Cui, Z. Chen, G. Li, and X. Chen, Macromol. Chem. Phys. **214**, 824 (2013).
65. T. Dong, Y. He, B. Zhu, A. Kyungmoo Shin, and Y. Inoue, Macromolecules **38**, 7736 (2005).
66. P. Pan, W. Kai, B. Zhu, A. Tungalag Dong, and Y. Inoue, Macromolecules **40**, 6898 (2007).
67. J. T. Kobayashi, T. Asahi, M. Ichiki, A. Oikawa, H. Suzuki, T. Watanabe, E. Fukada, and Y. J. Shikinami, Appl. Phys. **77**, 2957 (1995).
68. T. Kawai, N. Rahman, G. Matsuba, K. Nishida, T. Kanaya, M. Nakano, H. Okamoto, J. Kawada, A. Usuki, N. Honma, K. Nakajima, and M. Matsuda, Macromolecules **40**, 9463 (2007).
69. T. Fujiwara, T. Mukose, T. Yamaoka, H. Yamane, S. Sakurai, and Y. Kimura, Macromol. Biosci. **1**, 204 (2001).
70. P. Pan, B. Zhu, W. Kai, T. Dong, and Y. Inoue, J. Appl. Polym. Sci. **107**, 54 (2008).
71. J. Yang, T. Zhao, J. Cui, L. Liu, Y. Zhou, G. Li, E. Zhou, and X. Chen, J. Appl. Phys. **44**, 3215 (2006).
72. D. Zhou, J. Shao, G. Li, J. Sun, X. Bian, and X. Chen, Polymer **62**, 70 (2015).
73. D. W. Lim and T. G. Park, J. Appl. Polym. Sci. **75**, 1615 (2000).
74. D. Zhou, J. Shao, G. Li, J. Sun, X. Bian, and X. Chen, Polymer **62**, 70 (2015).
75. V. A. Belous, A. S. Kuprin, S. N. Dub, V. D. Ovcharenko, G. N. Tolmacheva, E. N. Reshetnyak, I. I. Timofeeva, and P. M. Litvin, J. Mech. Behav. Biomed. Mater. **17**, 242 (2013).
76. W. Kai, L. Zhao, B. Zhu, and Y. Inoue, Macromol. Chem. Phys. **207**, 746 (2006).
77. S. C. Tjong, J. S. Shen, and R. K. Y. Li, Polym. Eng. Sci. **36,** 100 (1996).
78. J. Karger-Kocsis, J. Varga, and G. W. Ehrenstein, J. Appl. Polym. Sci. **64**, 2057 (1997).
79. C. Grein, C. J. G. Plummer, H. H. Kausch, Y. Germain, and P. Béguelin, Polymer **43**, 3279 (2002).
80. N. Ljungberg and B. Wesslén, Polymer **44**, 7679 (2003).